Supplementary Information

Human CD24$^+$ dental papilla cells are highly competent seed cells for dentin-pulp regeneration via BMP2/SIRT1 metabolic axis

This PDF file includes:

Supplementary Figs 1 to 11.

Supplementary Table 1. Primer sequences used for quantitative RT-qPCR.

Supplementary Table 2. siRNA sequences.

Supplementary Figure 1:

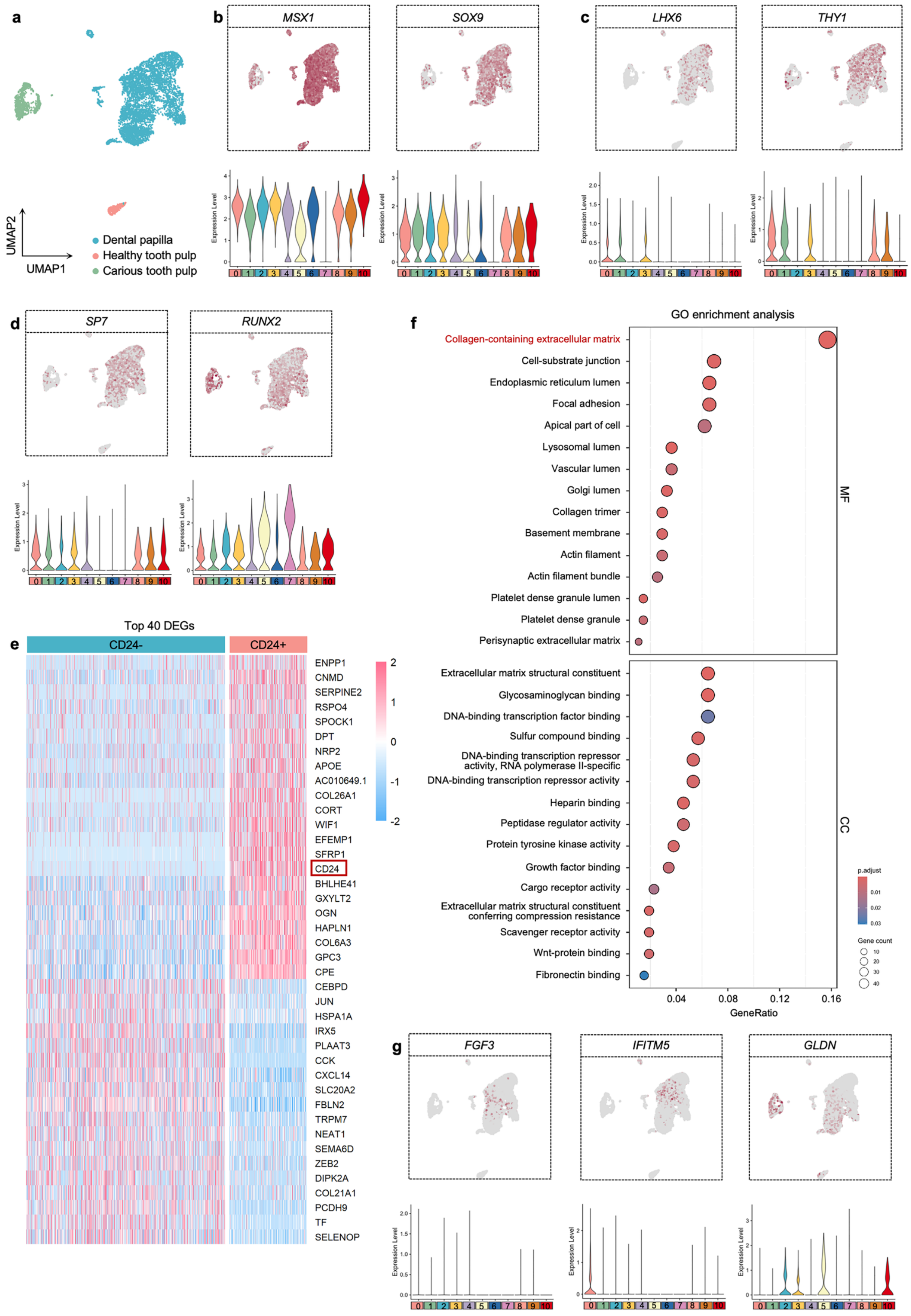

Supplementary Figure 1. Characterization of mesenchymal cell subsets by re-clustering analysis. a Integrated UMAP plot of DMCs across the dental papilla, adult tooth pulp, and carious tooth pulp in humans. **b–d** Feature (upper) and violin (below) plots of *MSX1*, *SOX9*, *LHX6*, *THY1*, *RUNX2*, and *SP7* expression in each cell cluster. **e** Heatmap of the top 40 DEGs between CD24$^+$ and CD24$^-$ subsets. **f** GO enrichment analysis of the top 15 enriched Molecular Functions (MF) and Cellular Component (CC) terms. **g** Feature plot of *FGF3*, *GLDN*, and *IFITM5* expression.

Supplementary Figure 2:

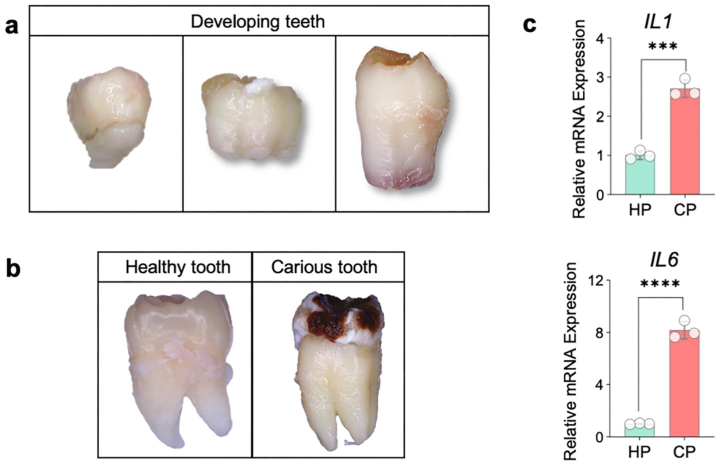

Supplementary Figure 2. Dental papilla and pulp samples from developing stage and carious conditions. a, **b** Representative tooth sample at different developing stages and carious state. **c** mRNA expression of *IL1* and *IL6* from pulp samples in (**b**). $n = 3$ per group. Data are mean ± SEM, $***P < 0.001$, $****P < 0.0001$, unpaired Student's *t*-test.

Supplementary Figure 3:

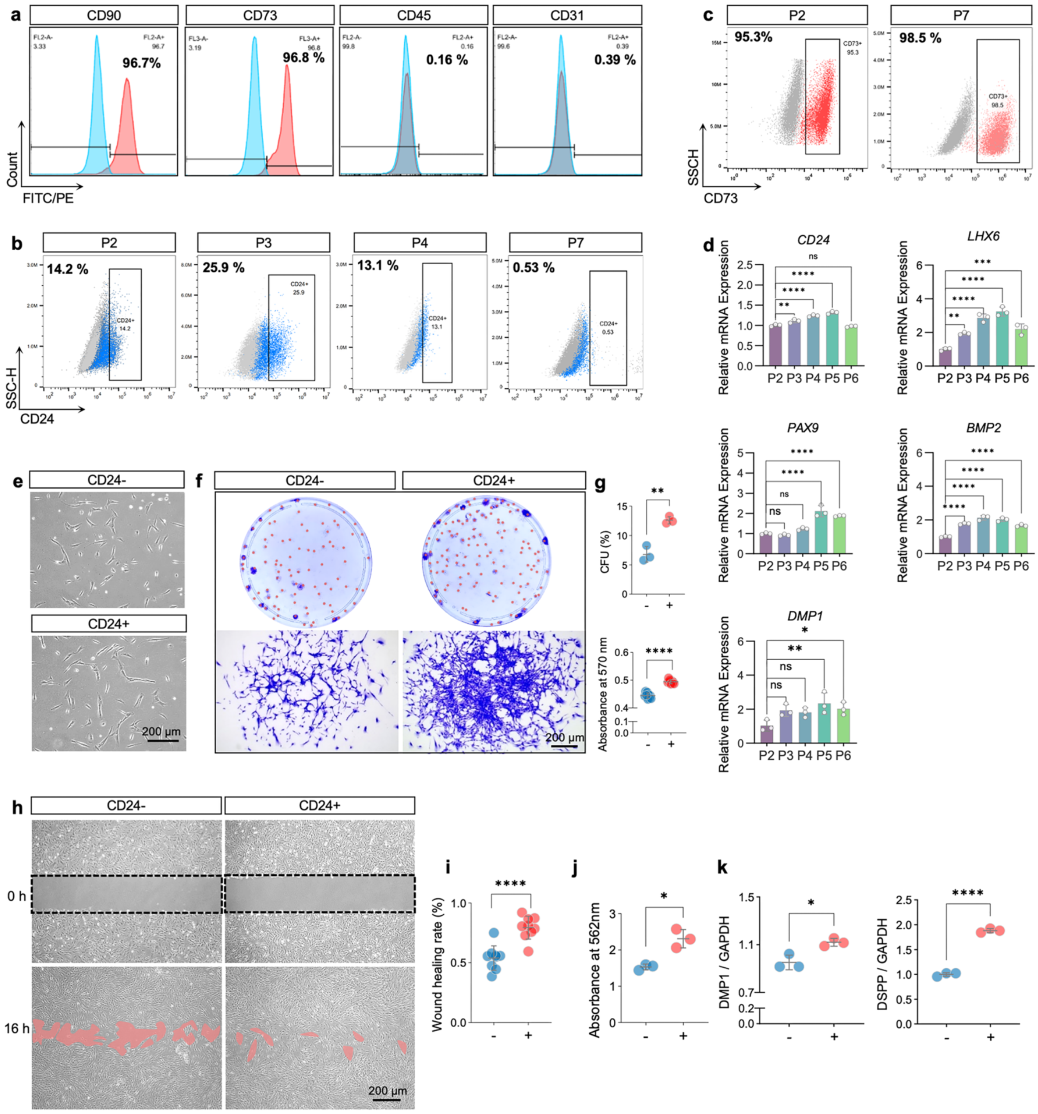

Supplementary Figure 3. Functional assessment of CD24$^+$ hDPCs in 2D culture system. **a** Flow cytometry analysis of CD90$^+$, CD73$^+$, CD45$^+$, and CD31$^+$ cell proportions in cultured hDPCs. **b**, **c** CD24$^+$ (**b**) and CD73$^+$ (**c**) cell proportions during serial passaging (P2–P7) in cultured hDPCs using flow cytometry. **d** mRNA expression of *CD24*, *LHX6*, *PAX9*, *BMP2*, and *DMP1* in cultured hDPCs during serial passaging (P2–P6). *n* = 3 per group. **e** Bright-field images showing the morphology of sorted CD24$^+$ and CD24$^-$ hDPCs. **f** Colony-forming assay of CD24$^+$ and CD24$^-$ hDPCs at day 10. Crystal violet staining showing the cell clusters. **g** Quantification of the colony-forming unit (CFU) and absorbance at 570 nm of crystal violet staining in (**f**). *n* = 3 per group. **h** Bright-field images showing the migration of CD24$^+$ and CD24$^-$ hDPCs by the scratch assay, cultured for 16 hours. The pink pseudo-color shows the unhealed area. **i** Quantification of wound healing rate in (**h**). *n* = 9 per group. **j** Quantification of Alizarin red staining by absorbance at 562 nm in Fig. 2f. **k** Quantification of DMP1 and DSPP expression in Fig. 2h. Data are mean ± SEM, $^*P < 0.05$, $^{**}P < 0.01$, $^{***}P < 0.001$, $^{****}P < 0.0001$, ns, not significant, unpaired Student's *t*-test (**g**, **i**–**k**) or one-way ANOVA followed by Tukey's test (**d**).

Supplementary Figure 4:

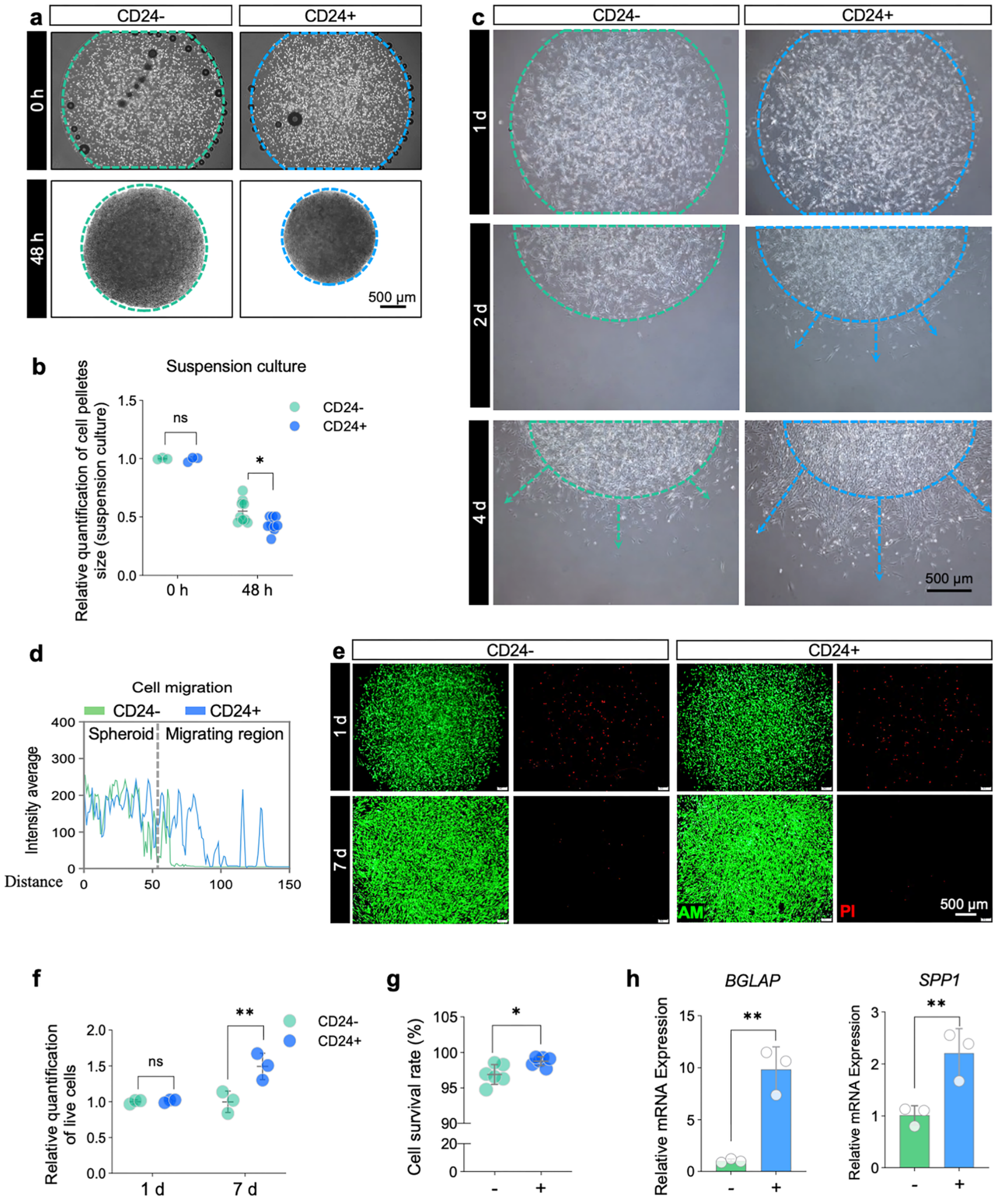

Supplementary Figure 4. Functional assessment of CD24$^+$ hDPCs in 3D culture system. a Bright-field images showing spheroid contraction of CD24$^+$ and CD24$^-$ hDPCs under high-density (4 × 10^6 cells/mL) suspension 3D culture conditions. 0 h represents culture initiation (baseline), and subsequent time points illustrate size changes during incubation. Dashed lines delineate the spheroid boundary. **b** Quantification of spheroid diameters in (**a**). *n* = 9 per group. **c** Bright-field fluorescent staining showing cell migration from low-density (2×10^6 cells/mL) spheroids in adherent 3D culture. Dashed lines delineate the spheroid boundary and radial migration direction. **d** Intensity profile of selected regions (white arrow line) in Fig. 2k. **e** Fluorescence microscopy images of $CD24^+$ and $CD24^-$ spheroids cultured under adherent 3D conditions for 1 day and 7 days. Live cells were stained with calcein AM (AM; green) and dead cells with propidium iodide (PI; red) to assess viability. **f**, **g** Quantification of live cell density (**f**, $n = 3$ per group) and cell viability (**g**, $n = 6$ per group) in (**e**). **h** mRNA expression of mineralization-related genes *BGLAP* and *SPP1* in Fig. 2m. Data are mean ± SEM, ns, not significant, $^*P < 0.05$, $^{**}P < 0.01$, unpaired Student’s *t*-test.

Supplementary Figure 5:

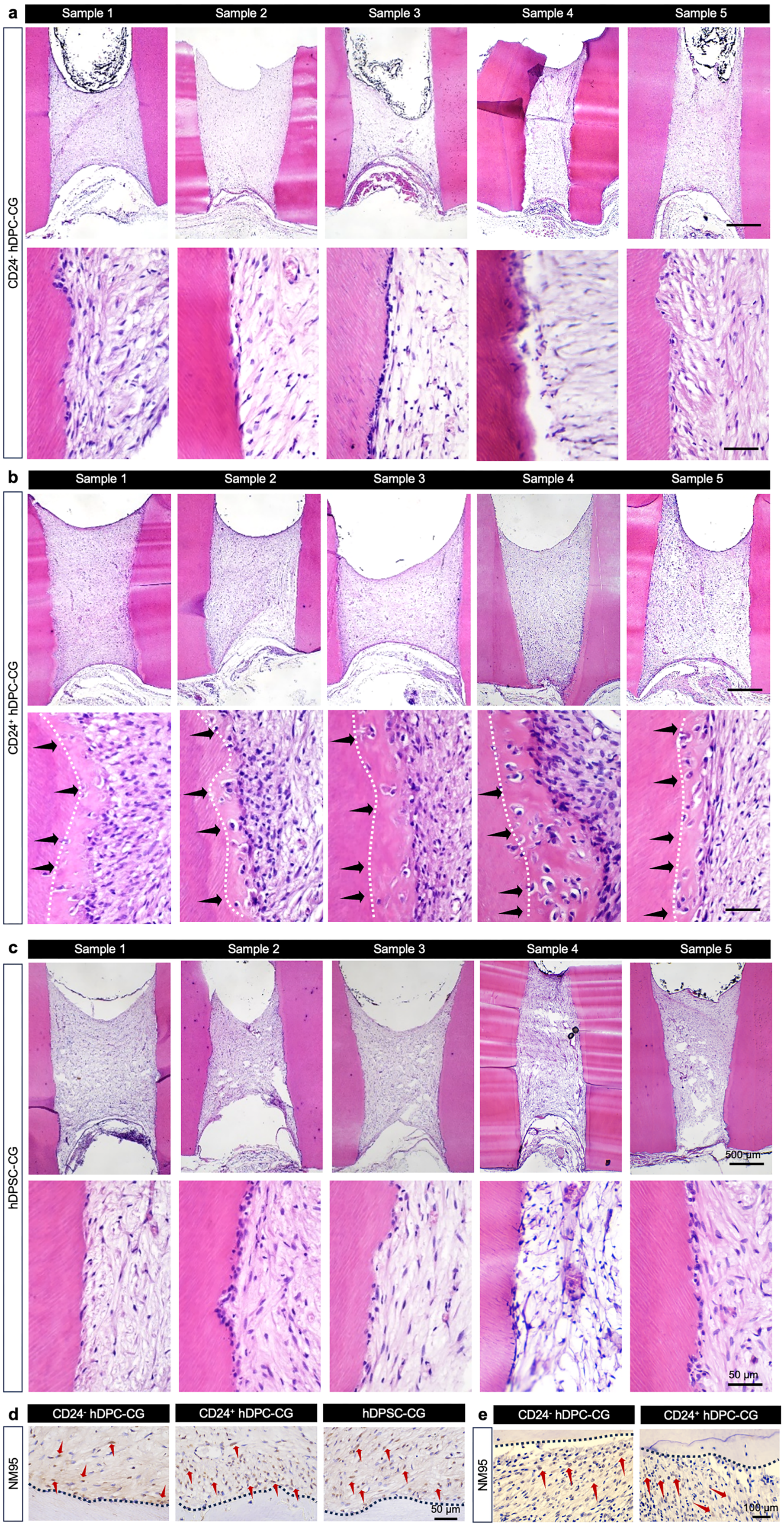

Supplementary Figure 5. CD24$^+$ hDPC CG mediates dentin-pulp complex regeneration. a–c H&E staining of regenerated dentin-pulp-like tissues at 4 weeks post-transplantation. White dashed lines show the tissue boundaries. Black arrows indicate regenerated dentin wall. $n = 5$ per group. **d**, **e** Immunohistochemical staining for human cell marker NM95 in regenerated pulp-like tissues of the murine (**d**) and the minipig (**e**) models. Black dashed lines show the tissue boundaries. Red arrows indicate NM95$^+$ cells.

Supplementary Figure 6:

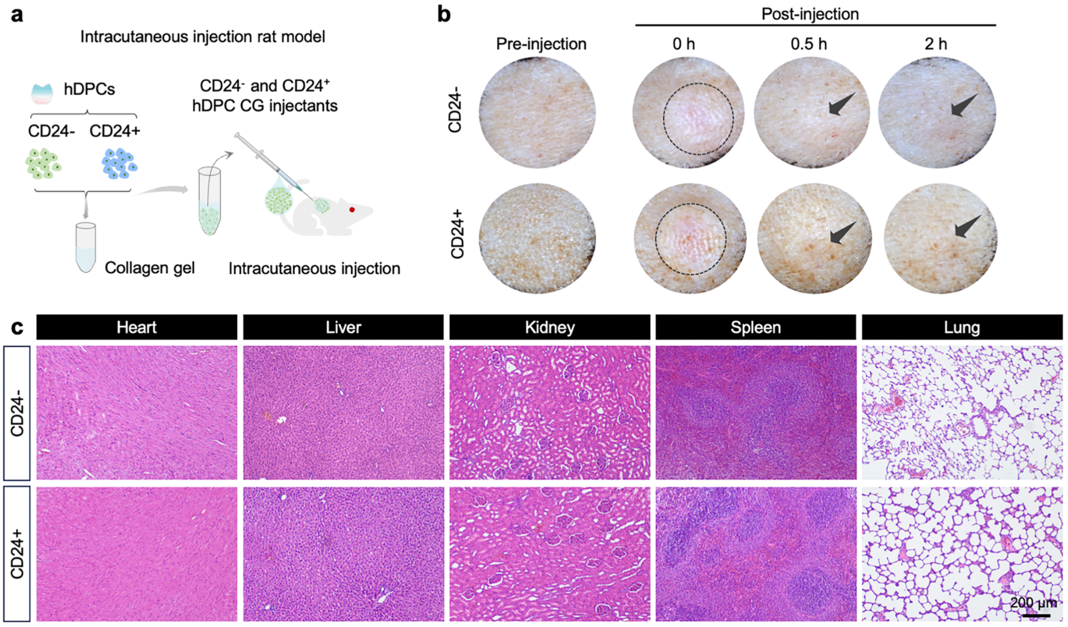

Supplementary Figure 6. Biosafety evaluation of CD24$^+$ and CD24$^-$ hDPC CG injectant. **a** Schematic illustrating the procedures of intracutaneous injection in immunocompetent rats. **b** Representative images of acute inflammatory responses at pre-injection, and 0, 0.5, and 2h post-injection. **c** H&E staining of major organs at 1 week post-injection.

Supplementary Figure 7:

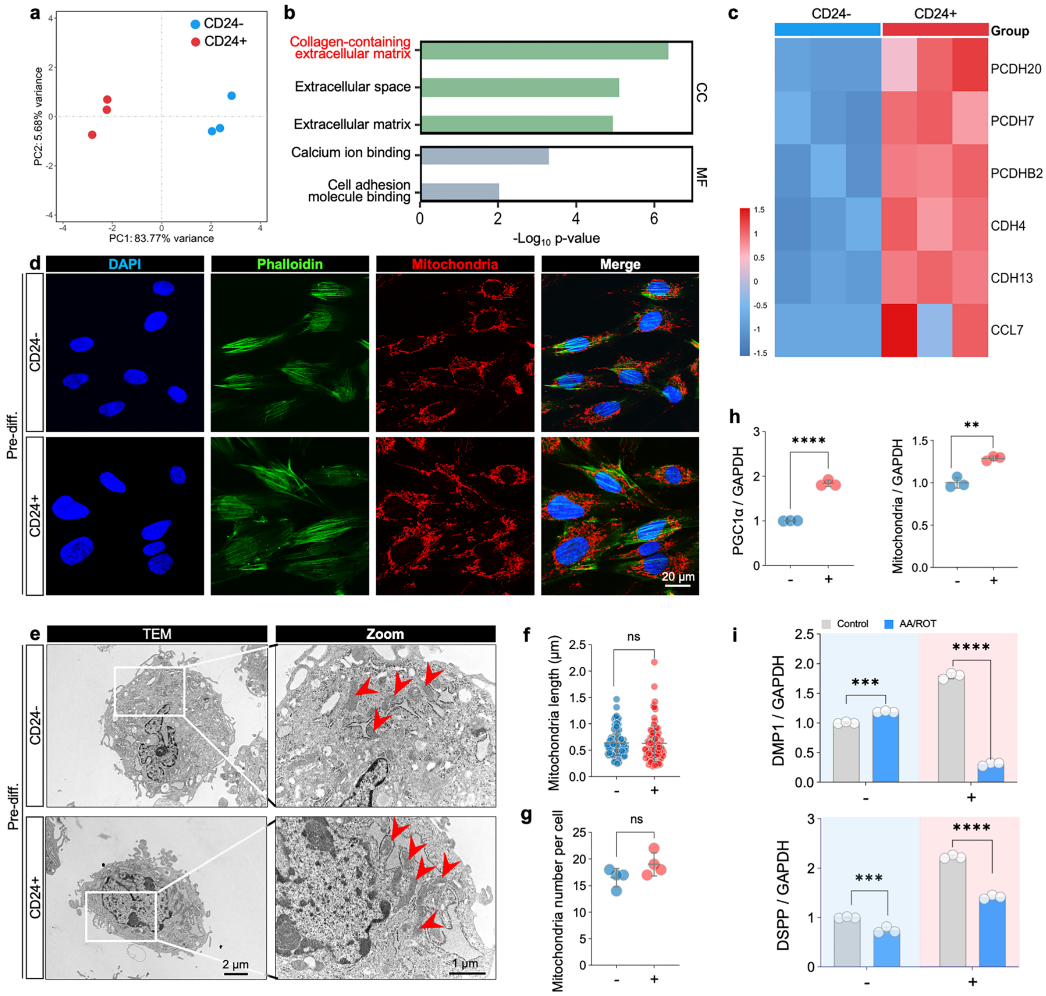

Supplementary Figure 7. Mitochondrial metabolic shift during CD24^{+} hDPCs lineage specification. a PCA showing distinct transcriptomic profiles between cultured CD24^{+} and CD24^{-} hDPCs. **b** GO analysis showing enriched MF and CC terms. **c** Heatmap of the differential genes of cadherin and chemokine families in CD24^{+} and CD24^{-} hDPCs. **d** Immunofluorescence imaging of mitochondria distribution in cultured CD24^{+} and CD24^{-} hDPCs before induction. **e** TEM images showing mitochondrial morphology (indicated by red arrowheads) in CD24^{+} and CD24^{-} hDPCs before induction. **f**, **g** Quantification of mitochondrial length (*n* = 90 per group) and number per cell (*n* = 4 per group) from TEM images in (**e**). **h** Quantification of PGC1α expression and mitochondrial protein content in Fig. 4o. **i** Quantification of DMP1 and

DSPP expression in Fig. 4q. **j** mRNA expression for *PPARGC1A* and *TFAM* in $CD24^+$ hDPCs treated with AA/ROT. $n = 3$ per group. Data are mean ± SEM, $^{**}P < 0.01$, $^{***}P < 0.001$, $^{****}P < 0.0001$, ns, not significant, unpaired Student's *t*-test.

Supplementary Figure 8:

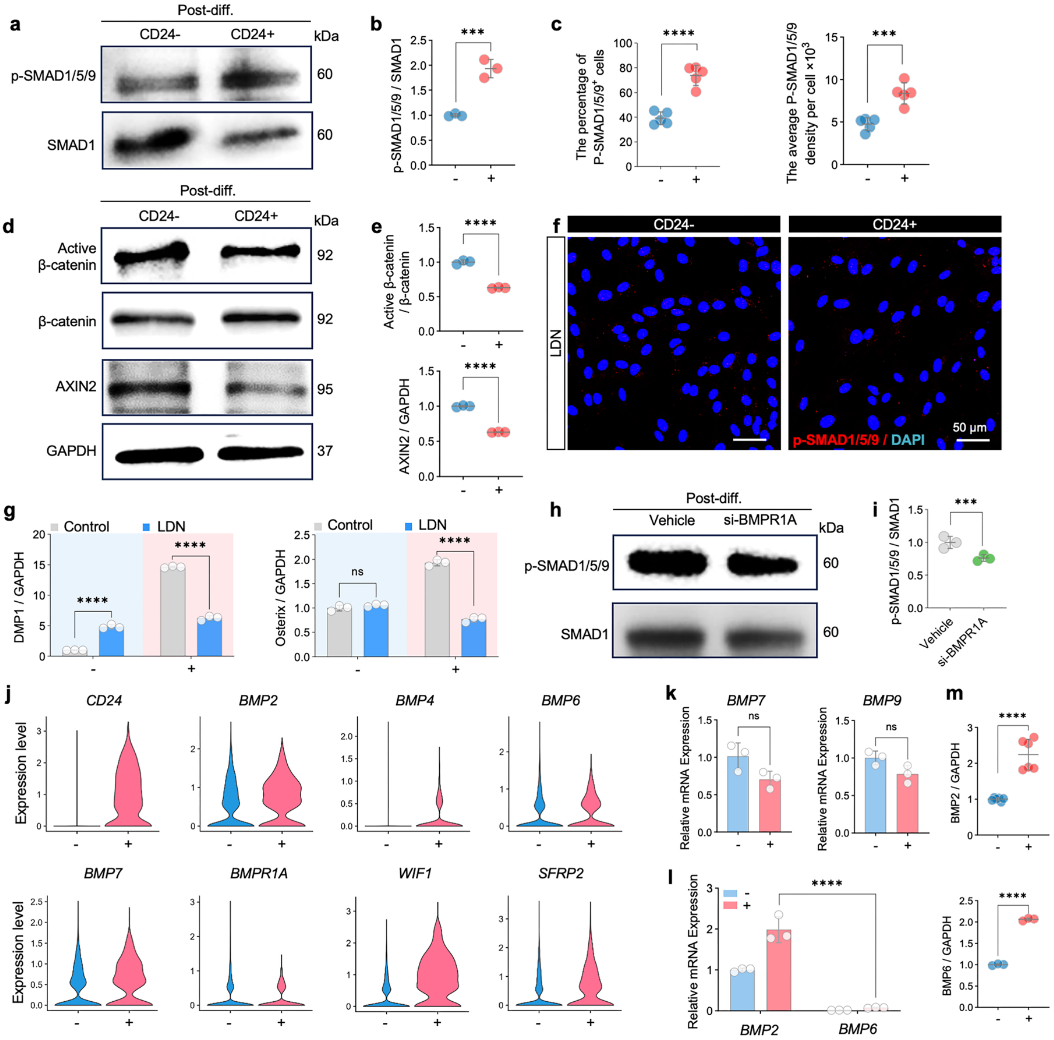

Supplementary Figure 8. BMP signaling activation during odontogenic differentiation of CD24$^+$ hDPCs. **a** Immunoblotting for p-SMAD1/5/9 expression in CD24$^+$ and CD24$^-$ hDPCs under induction. *n* = 3 per group. **b** Quantification of p-SMAD1/5/9 expression in (**a**). **c** Quantification of p-SMAD1/5/9$^+$ cell proportion and signal intensity per cell in Fig. 5a. *n* = 5 per group. **d** Immunoblotting for active β-catenin, β-catenin, and AXIN2 expression in induced CD24$^+$ and CD24$^-$ hDPCs. *n* = 3 per group. **e** Quantification of indicated protein levels in (**d**). **f** Immunofluorescent staining for p-SMAD1/5/9 in CD24$^+$ and CD24$^-$ hDPCs induced with LDN193189. **g** Quantification of DMP1 and OSX expression in Fig. 5g. **h** Immunoblotting for p-

SMAD1/5/9 expression with or without siRNA-mediated knockdown of *BMPR1A* in CD24$^+$ hDPCs. $n = 3$ per group. **i** Quantification of p-SMAD1/5/9 protein level in (**h**). **j** Violin plots of *CD24, BMP2*, *BMP4*, *BMP6*, *BMP7*, *BMPR1A*, *WIF1*, and *SFRP2* expression in CD24$^+$ and CD24$^-$ subsets. **k** mRNA expression of *BMP7* and *BMP9* in cultured CD24$^+$ and CD24$^-$ hDPCs. $n = 3$ per group. **l** mRNA expression of *BMP2* and *BMP6*. $n = 3$ per group. **m** Quantification of BMP2 and BMP6 protein levels in Fig. 5s. Data are mean ± SEM, $^{***}P < 0.001$, $^{****}P < 0.0001$, ns, not significant, unpaired Student's *t*-test.

Supplementary Figure 9:

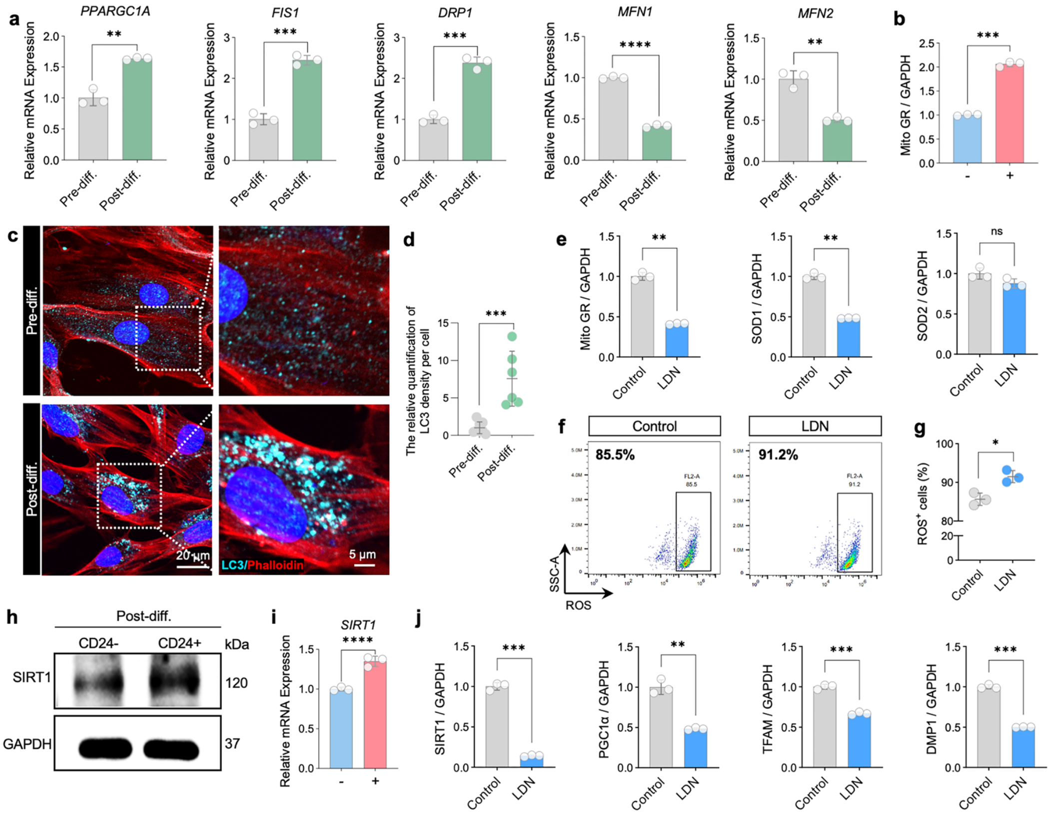

Supplementary Figure 9. BMP/SIRT1-mediated regulatory network in odontogenic differentiation of CD24$^+$ hDPCs. **a** mRNA expression of *PPARGC1A*, *FIS1*, *DRP1*, *MFN1*, and *MFN2* in induced CD24$^+$ hDPCs. *n* = 3 per group. **b** Quantification of mito GR expression level in Fig. 6f. **c** Immunofluorescent staining for LC3 in CD24$^+$ hDPCs before and after induction. **d** Quantification of LC3 fluorescence intensity in (**c**). *n* = 6 per group. **e** Quantification of Mito GR, SOD1, and SOD2 expression levels in Fig. 6i. **f** Flow cytometry showing ROS level in CD24$^+$ hDPCs induced with or without LDN193189. *n* = 3 per group. **g** Quantification of ROS$^+$ cell proportion in (**f**). **h** Immunoblotting for SIRT1 expression in induced CD24$^+$ and CD24$^-$ hDPCs. *n* = 3 per group. **i** Quantification of SIRT1 expression level in (**h**). **j** Quantification of SIRT1, PGC1α, TFAM, and DMP1 expression in Fig. 6q. Data are mean ± SEM, $^*P < 0.05$, $^{**}P < 0.01$, $^{***}P < 0.001$, $^{****}P < 0.0001$, ns, not significant, unpaired Student's *t*-test.

Supplementary Figure 10:

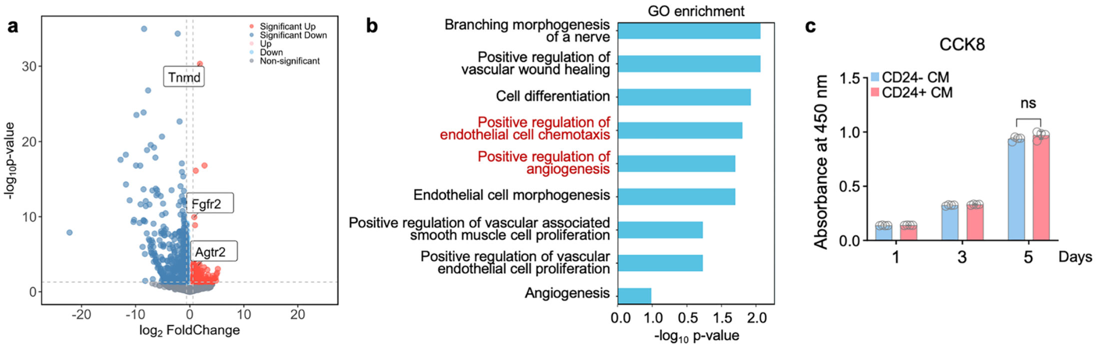

Supplementary Figure 10. The pro-angiogenic capacity of CD24$^+$ hDPCs. a Volcano plot showing DEGs of transcriptomic analysis in regenerated tissues between CD24$^+$ and CD24$^-$ groups within the ectopic model, at two weeks post-transplantation. **b** GO analysis visualizing the enriched angiogenesis-related terms in the CD24$^+$ group. **c** CCK8 assay evaluating proliferation capability of HUVEC under CD24$^+$ or CD24$^-$ hDPC-derived CM treatment. *n* = 4 per group. Data are mean ± SEM, ns, not significant, unpaired Student’s *t*-test.

Supplementary Figure 11:

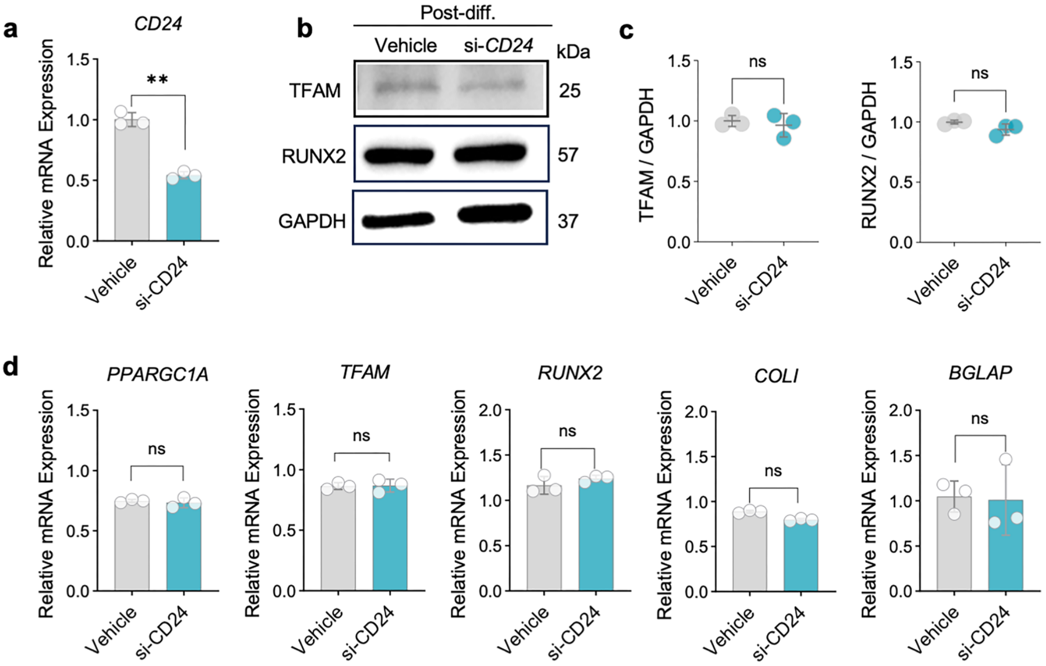

Supplementary Figure 11. Regulatory role of the *CD24* gene in CD24^{+} hDPCs. a mRNA expression of *CD24* in CD24^{+} hDPCs treated with or without *CD24* siRNA. *n* = 3 per group. **b** Immunoblotting for *TFAM* and *RUNX2* expression in induced CD24^{+} hDPCs treated with *CD24* siRNA. *n* = 3 per group. **c** Quantification of indicated protein levels in (**b**). **d** mRNA expression of *PPARGC1A*, *TFAM*, *RUNX2*, *COLI*, and *BGLAP* in CD24^{+} hDPCs treated with *CD24* siRNA. *n* = 3 per group. Data are mean ± SEM, $^{**}P < 0.01$, ns, not significant, unpaired Student's *t*-test.

Supplementary Table 1: Primer sequences used for quantitative RT-PCR.

Gene	**Forward**	**Reverse**
CD24	CTCCATTCCACAATCCCATC	GAAGGAGAGGCAACATCCAA
LHX6	GCTCTGCCGCATCCACTACG	TTGGGTTGACTGTCCTGTTCCG
PAX9	GCTCCATCACCGACCAAGT	CTCCCTTCTCCAACCCGTTC
RUNX2	CTTTACTTACACCCCGCCAGTC	AGAGATATGGAGTGCTGCTGGTC
ALP	TAAGGACATCGCCTACCAGCTC	TCTTCCAGGTGTCAACGAGGT
DSPP	CGACATAGGTCACAATGAGGATGTCG	TTGCTTCCAGCTACTTGAGGTC
DMP1	AGCATCCTGCTCATGTTCCTT	TGATGACTCACTGCTCTCCAAG
OCN	CTCACACTCCTCGCCCTATT	CCTCCTGCTTGGACACAAA
OPN	CAGTTGTCCCCACAGTAGACAC	GTGATGTCCTCGTCTGTAGCATC
COLI	AACATGGAGACTGGTGAGACCT	CGCCATACTCGAACTGGAATC
IL1	CTTTGAAGCTGATGGCCCTAAA	AGTGGTGGTCGGAGATTCGT
IL6	TGTGAAAGCAGCAAAGAGGC	TGGGTCAGGGGTGGTTATT
BMP2	AACAATGGCATGATTAGTGG	CAGACGGGAGTTTCTCCTCGGACGT
BMP6	GCTCAACCGCAAGAGCCTTC	TGTCGTACTCCACCAGGTTC
BMP7	GACTTCAGCCTGGACAACGA	AGGTCCAGCATGAACATGGG
BMP9	AGGTGAGAGCAGTCACGAG	CGTCACATCGTCAGCCAAG
BMPR1A	CCTGTTGTCATAGGTCCGTTTT	ATCCTGTTCCAAATCACGATTGT
SFRP2	ATGATGATGACAACGACATAATG	ATGCGCTTGAACTCTCTCTGC
WIF1	TCTCCAAACACCTCAAAATGCT	GACACTCGCAGATGCGTCT
SIRT1	AGAACTTCAGTGGCTGGAACAGTG	CCATCAAGCCGCCTACTAATCTGC
PGC1α	TCTGAGTCTGTATGGAGTGACAT	CCAAGTCGTTCACATCTAGTTCA
TFAM	ATGGCGTTTCTCCGAAGCAT	TCCGCCCTATAAGCATCTTGA
NRF1	AGGAACACGGAGTGACCCAA	TATGCTCGGTGTAAGTAGCCA
FIS1	GATGACATCCGTAAAGGCATCG	AGAAGACGTAATCCCGCTGTT
DRP1	CTGCCTCAAATCGTCGTAGTG	GAGGTCTCCGGGTGACAATTC
MFN1	TGGCTAAGAAGGCGATTACTGC	TCTCCGAGATAGCACCTCACC
MFN2	CTCTCGATGCAACTCTATCGTC	TCCTGTACGTGTCTTCAAGGAA
SOD1	TCATCAATTTCGAGCAGAAGG	CAGGCCTTCAGTCAGTCCTTT
SOD2	GGAAGCCATCAAACGTGACTT	CCCGTTCCTTATTGAAACCAAGC
VEGF	AGGGAAGAGGAGGAGATGAG	GCTGGGTTTGTCGGTGTT

Supplementary Table 2: siRNA sequences.

Gene	**Sequences**
si*CD24* (human)	5'-GCAGTCAACAGCCAGTCTCTT-3'
si*BMPR1A* (human)	5'-GCTGTCTGCATAATTGCTATG-3'
si*Cd24* (mouse)	5'-GAUUAAAGGACGCGUGAAATT-3'